

Simulation of textures and Lankford values for face centered cubic polycrystalline metals by using a modified Taylor model

A. Ma, F. Roters, D. Raabe

*Max-Planck-Institut für Eisenforschung
Max-Planck-Str. 1
40237 Düsseldorf
Germany*



For further details please contact: raabe@mpie.de or roters@mpie.de



ABSTRACT

This report presents a modified Taylor model is presented which statistically considers grain interaction in a polycrystalline aggregate in terms of a standard deviation for the symmetric part of the velocity gradient. The model can be solved using a Newton iteration method. We simulate crystallographic rolling textures and the anisotropy arising from uniaxial tension tests (Lankford values for different directions in the rolling sheet plane). The results reveal in part a good agreement with experimental data.

Keywords texture, anisotropy, r-value, micromechanical modelling, rolling, plastic deformation, FCC metals, simulation



1 Introduction

1.1 Motivation for this texture study

Crystalline engineering materials mostly occur in polycrystalline forms where each grain has a different crystallographic orientation, shape, and volume fraction. The distribution of the grain orientations is referred to as crystallographic texture. The discrete nature of crystallographic slip along certain lattice directions on preferred crystallographic planes together with the occurrence of pronounced textures with certain preferred orientations entail an overall highly anisotropic elastic-plastic response of such polycrystalline samples under mechanical loads.

An important aim of polycrystal research consists in developing mechanical models for understanding and predicting the evolution of texture and crystalline anisotropy particularly at large plastic strains. In this context mechanical homogenization models (such as Taylor-type models) play an important role due to their considerable success in providing in part excellent texture approximations on the basis of relatively simple and, therefore, computationally very efficient constitutive concepts [for overviews see 1-5].

The current study is concerned with the introduction of a modified Taylor model which considers grain interaction in a polycrystalline aggregate in a statistical fashion by introducing a standard deviation for the symmetric part of the imposed velocity gradient. We use it for the simulation of rolling textures and Lankford values of face centered cubic (FCC) metals.

1.2 Fundamentals of plasticity homogenization models for textured polycrystals

Two early versions of texture homogenization models were proposed by Sachs [6] and Taylor [7]. The Sachs model is a no-strain-constraints (NC) model in which the external stresses are considered homogeneous for each individual grain of a polycrystalline aggregate. Since it neglects strain compatibility the Sachs model represents a lower-bound result for the stresses of a mechanically loaded polycrystalline sample [3]. The Taylor model is a full-strain-constraints (FC) approach in which the external strains are equally valid for each single grain. Since it neglects



stress equilibrium the Taylor model represents an upper-bound result for the strains of a polycrystal [3].

Early modifications of this full-constraints Taylor model were introduced by incorporating strain relaxations between neighboring grains, leading to the so called relaxed-constraints Taylor model variants (RC models) [8-11]. In these approaches some of the external shear components are not transferred into the grain, i.e. the RC models allows for shear strains at the grain-scale. A relaxation of the strain component ε_{13} corresponds to a shear in longitudinal direction (so called *lath* RC model), while ε_{23} denotes the transverse shear. The relaxation of both ε_{13} and ε_{23} is referred to as *pancake* RC model. Allowing relaxations for these shears locally leads to distinct changes in the reorientation rates and, therefore, in the texture development when compared to the predictions of the FC Taylor model. Although the texture predictions obtained by RC models principally yield better results than those of the NC or FC approaches, deviations were observed particularly in the large strain regime.

Therefore, different approaches were suggested to render the classical Taylor or Sachs homogenization models physically more plausible and in better accord with experimental data. Conceptual modifications of the constitutive descriptions consist essentially in the introduction of grain-interactions or respectively interaction penalty measures as well as in strain relaxation schemes which depend on the corresponding gain in the deformation energy resulting from certain types and amounts of strain relaxations. These terms quantify the elastic-plastic mismatch between neighboring grains or within larger grain clusters where the interacting grains are typically selected statistically from a large set of single orientations which map the inherited texture. Details about these model variants can be found in [12-18].

Similar efforts were made for instance by Mao [19] to modify the Sachs model. He calculated the deformation by activating primary slip and assuming shear strain impediment in terms of back stresses generated by the surrounding grains. In this modified Sachs model the induced reaction stresses may entail the activation of additional slip systems which compensate for the primary deformation. Related concepts are the self-consistent polycrystal models [e.g. 20]. In these approaches each crystal is treated as an elastic-plastic inclusion which is embedded in an otherwise homogeneous effective medium which has the average properties of the polycrystal. Self-consistent polycrystal models are solved in an iterative fashion for the deformation and the stress. Although



self-consistent models satisfy both, strain compatibility and stress equilibrium at the same time they represent one-site approximations. Modifying them into N-site approximations by consideration of some local neighborhood would render them less efficient.

Based on the Taylor model, a neighborhood compliance model was suggested by Sarma and Dawson [21]. In this model a neighborhood is determined for every single crystal, which contains a certain number of crystals around this main single crystal. A new compliance tensor for each single crystal embedded in such a grain cluster can be determined through a Taylor calculation and a local stress homogenization procedure. This early approach of Sarma and Dawson to explicitly incorporate grain neighborhood effects into texture models inspired our current study in which we introduce a statistical neighborhood for each grain of a polycrystal through a pseudorandom function imposed for the velocity gradient tensor.

1.3 Basic introduction to the crystallographic textures of rolled FCC metals

Owing to the cubic symmetry of the FCC crystal system and the orthorhombic sample system which is set up by the rolling direction (RD), normal direction (ND), and transverse direction (TD) of the sample, textures of rolled FCC polycrystals are typically presented in the reduced Euler space where an orientation is given by the three Euler angles φ_1 , ϕ , and φ_2 , ($0^\circ \leq \varphi_1, \phi, \varphi_2 \leq 90^\circ$). We use the Bunge notation for the Euler angles throughout this report [22]. Crystal orientations can also be conveniently described by the use of Miller indices $\{hkl\}\langle uvw \rangle$. In this concept the triple $\{hkl\}$ describes the crystallographic plane parallel to the sheet surface whereas $\langle uvw \rangle$ indicates the crystal direction parallel to RD.

Important texture components are on the α_{fcc} -fiber which comprises all orientations with a common crystallographic fiber axis $\langle 011 \rangle$ parallel to the normal direction including major components $\{011\}\langle 100 \rangle$ (Goss-component, $\varphi_1=0^\circ$, $\phi=45^\circ$, $\varphi_2=0^\circ$), $\{0\bar{1}1\}\langle 211 \rangle$ (Brass-component, $\varphi_1=35^\circ$, $\phi=45^\circ$, $\varphi_2=0^\circ$), $\{0\bar{1}1\}\langle 111 \rangle$, and $\{0\bar{1}1\}\langle 011 \rangle$ (90° about the normal rotated Goss-component, $\varphi_1=90^\circ$, $\phi=45^\circ$, $\varphi_2=0^\circ$) and the less symmetric β -skeleton line including major



components $\{211\}\langle 111 \rangle$ (Copper-component, $\varphi_1=90^\circ$, $\phi=35^\circ$, $\varphi_2=45^\circ$), $\{123\}\langle 634 \rangle$ (S-component, $\varphi_1=60^\circ$, $\phi=32^\circ$, $\varphi_2=65^\circ$), and the Brass component $\{011\}\langle 211 \rangle$ ($\varphi_1=35^\circ$, $\phi=45^\circ$, $\varphi_2=0^\circ$) [1,2,4,8,9,23-25].

1.4 Macroscopic parameters for plastic sheet anisotropy

Sheet rolling is related to a plane-strain compression process [1-4, 26]. The plastic anisotropy of a rolled sheet is typically characterized in terms of the Lankford coefficient [27] or R -value, which is defined as the ratio of the width plastic strain, ε_W^P , to the through-thickness plastic strain, ε_T^P , i.e.

$$R = \varepsilon_W^P / \varepsilon_T^P \quad (1.1)$$

Although this simple definition offers at first view an adequate and straightforward means for assessing the in-plane and through-thickness flow and shape anisotropy of sheets, experiments reveal that the R -value shows a significant strain dependence even at very small strains [2-4,28-30]. As additional parameters Kocks et al. [4] have suggested to use the ratio of the width component of the strain rate, \mathbf{D} , to its through-thickness component, i.e.

$$r = D_W / D_T \quad (1.2)$$

and the ratio of the width component of the strain rate to the length component

$$q = D_W / D_L \quad (1.3)$$

Mathematically, the latter parameter q is a very helpful one because it will not vary from 0 to infinity as the conventional r parameter.

Another parameter for the quantification of the sheet resistance against thinning and its anisotropy was suggested by Spolidor [30] as



$$\rho = \frac{dy}{dx} \frac{x}{y} \quad (1.4)$$

where x and y are the *actual* thickness and the width of the specimen, respectively. This parameter is designed to take into account the change of the loading path during a mechanical test. Taking an empirical theoretical perspective Rees [26] has developed an analytical function for the evolution of the r -value during straining which, however, is based on the assumption that the rolling anisotropy can be expressed by Hill's yield function. In our study we choose the q -parameter to study the planar anisotropy of rolled FCC sheets.

2 Constitutive equations for conventional elastic-plastic Taylor modeling

2.1 Elastic rule

Based on the isomorphy assumption [31], the actual elastic law of a single crystal can be represented by the referential elastic law through a plastic transformation \mathbf{P} . The elastic law for the current configuration is

$$\mathbf{T}^{2PK} = \mathbf{P}\tilde{\mathbf{K}}\left[\frac{1}{2}(\mathbf{P}^T\mathbf{C}\mathbf{P} - \mathbf{I})\right]\mathbf{P}^T \quad (2.1)$$

$$\mathbf{C} = \mathbf{F}^T\mathbf{F} \quad (2.2)$$

where \mathbf{F} is the deformation gradient, \mathbf{T}^{2PK} is the second Piola-Kirchhoff stress tensor, \mathbf{C} is the right Cauchy-Green strain tensor, \mathbf{I} is the second order identity tensor, and the fourth order tensor $\tilde{\mathbf{K}}$ is the elasticity tensor with respect to the undistorted configuration. From equation (2.1), the Cauchy stress \mathbf{T} can be calculated as

$$\mathbf{T} = \frac{1}{\tilde{J}}\tilde{\mathbf{F}}\tilde{\mathbf{K}}\left[\frac{1}{2}(\tilde{\mathbf{F}}^T\tilde{\mathbf{F}} - \mathbf{I})\right]\tilde{\mathbf{F}}^T \quad (2.3)$$



with

$$\tilde{\mathbf{F}} = \mathbf{F}\mathbf{P} \quad (2.4)$$

and

$$\tilde{J} = \det(\tilde{\mathbf{F}}) . \quad (2.5)$$

2.2 Flow rule

The velocity gradient $\mathbf{L} = \dot{\mathbf{F}}\mathbf{F}^{-1}$ is used to express the deformation process. Using equation (2.4) it can be expressed as

$$\mathbf{L} = \dot{\tilde{\mathbf{F}}}\tilde{\mathbf{F}}^{-1} + \tilde{\mathbf{F}}\mathbf{L}_p\tilde{\mathbf{F}}^{-1} \quad (2.6)$$

$$\mathbf{L}_p = -\mathbf{P}^{-1}\dot{\mathbf{P}} . \quad (2.7)$$

Using $\tilde{\mathbf{d}}_\alpha$ for the slip direction and $\tilde{\mathbf{n}}_\alpha$ the slip plane normal direction with respect to the undistorted configuration, one obtains the dyadic product $\tilde{\mathbf{M}}_\alpha = \tilde{\mathbf{d}}_\alpha \otimes \tilde{\mathbf{n}}_\alpha$ as the Schmid tensor for the slip system α . For FCC crystals we assume slip to occur on the 12 octahedral systems $\{111\}\langle 110\rangle$. The plastic portion of the velocity gradient, \mathbf{L}_p , can then be formulated as

$$\mathbf{L}_p = \sum_{\alpha=1}^{12} \dot{\gamma}_\alpha \tilde{\mathbf{M}}_\alpha \quad (2.8)$$

with

$$\dot{\gamma}_\alpha = \dot{\gamma}_0 \operatorname{sign}(\tau_\alpha) \left| \frac{\tau_\alpha}{\tau_\alpha^D} \right|^{\frac{1}{m}} . \quad (2.9)$$

The viscoplastic rule given by equation (2.9) is used to calculate the individual shear rates. In this expression $\dot{\gamma}_0$ is the reference shear rate, m is the strain rate sensitivity, τ_α^D the drag stress, and τ_α is the resolved shear stress of slip system α , which can be approximated by

$$\tau_\alpha \approx \tilde{\mathbf{K}} \left[\frac{1}{2} (\tilde{\mathbf{F}}^T \tilde{\mathbf{F}} - \mathbf{I}) \right] \cdot \tilde{\mathbf{M}}_\alpha \quad (2.10)$$



3 Constitutive equations for the modified Taylor model

The shortcoming of the classical Taylor model consists in the disregard of elastic-plastic grain interaction. Sarma and Dawson [21] assumed in their analysis that for one crystal which is embedded in an aggregate of 1000 grains only about 20 neighboring grains will influence the strain rate and stress of that crystal. This means that a relatively small set of grains suffices to compose a neighborhood for a grain in a polycrystal.

Sarma and Dawson showed that for the case of an isotropic texture the various components of the deformation rates of all individual grains in the aggregate establish normal distributions about the mean value [21]. For the case of a plane strain compression texture Sarma and Dawson observed a skewness of the normal distribution. These theoretical results on the heterogeneity in the grain-to-grain distribution of the accumulated plastic strains in mechanically loaded polycrystals were recently confirmed by experiment [32-33].

In our present approach we adopt these observations of Sarma and Dawson for the formulation of a modified Taylor approach. Since we aim at preserving the concept of the classical Taylor models, namely, to treat each grain in an isolated fashion without explicit incorporation of a local grain neighborhood, we introduce (positive and negative) standard deviations from the mean value for each component of the local velocity gradient tensor. In our model we assume that the deviation distribution can be expressed in terms of a pseudorandom function for all strain rate components. We also assume that the local velocity gradient is of the same principal type as the external one, the only difference being the pseudorandom distribution for each tensor component.

Using the pseudorandom number function $f(iseed)$ the local velocity gradient tensor \mathbf{L} of each single grain can be modified based on the formulation for the global velocity gradient, $\bar{\mathbf{L}}$, according to

$$L_{ij} = \bar{L}_{ij} + SD \times f(iseed) \quad (3.1)$$

$$\mathbf{L} = \bar{\mathbf{L}} - \frac{1}{3} tr(\bar{\mathbf{L}}) \mathbf{I} . \quad (3.2)$$

In expression (3.1) SD is the standard deviation and $iseed$ is the seed for the random number



generator. A similar approach was recently suggested by Engler [34] who introduced with considerable success statistical variations of the strain rate state into a Taylor model.

4 Numerical modelling of sheet rolling

4.1 Sheet rolling kinematics and material constants

Sheet rolling can be idealized as a plain strain compression state. Let the base vector \mathbf{e}_1 be in the compression direction (ND), \mathbf{e}_2 in the transverse direction (TD), and \mathbf{e}_3 in the rolling direction (RD). Plane strain compression can then be approximated by the following isochoric motion

$$\mathbf{x} = (\exp(\bar{L}_{11}t)\mathbf{e}_1 \otimes \mathbf{e}_1 + \exp(\bar{L}_{33}t)\mathbf{e}_3 \otimes \mathbf{e}_3)[\mathbf{X}] \quad (4.1)$$

In the present case we used $\bar{L}_{11} = -0.00707$ and $\bar{L}_{33} = -\bar{L}_{11}$. The material was assumed as OFHC copper with the elastic constants $\tilde{K}_{1111} = 168 \text{ GPa}$, $\tilde{K}_{1122} = 121 \text{ GPa}$, $\tilde{K}_{1212} = 75 \text{ GPa}$, $\tau_0^D = 16 \text{ MPa}$.

Further constants were $\dot{\gamma}_0 = 0.001 \frac{1}{s}$, $m = 0.012$.

4.2 Simulation of the unloading process

The aim of the unloading simulation consists in a relaxation step which reduces the macroscopic Cauchy stress to zero. The velocity gradient tensor for unloading is obtained as follows. First, the macroscopic stiffness tensor, $\bar{\mathbf{K}}$, is used for calculating the compliance tensor $\bar{\mathbf{S}}_U$ for the unloading,

$$\bar{\mathbf{S}}_U = (\bar{\mathbf{K}})^{-1} \quad (4.2)$$



Second, the compliance is used for calculating the unloading deformation, $\bar{\mathbf{E}}_U$, according to

$$\bar{\mathbf{E}}_U = \bar{\mathbf{S}}_U[\bar{\mathbf{T}}] . \quad (4.3)$$

Finally, the unloading velocity gradient tensor is assumed to be parallel to the unloading deformation

$$\mathbf{L}_U \parallel \bar{\mathbf{E}}_U \quad (4.4)$$

The beginning of the first unloading stage is not purely elastic, i.e. the macroscopic stress cannot directly relax to zero during unloading. Hence, a second unloading step is required to reach complete unloading. In this study more than two unloading steps are used to unload and relax the macroscopic Cauchy stress.

5 Taylor-based simulation of uniaxial tension testing for polycrystals

Classical variants of the Taylor model use the velocity gradient to describe the loading process, i.e. in terms of their boundary conditions they are models which are strictly *deformation controlled*. The uniaxial tension test, however, is a *stress* controlled process, which contradicts the basic approach taken by Taylor models. In the following we show how one can circumvent this problem and conduct a Taylor-based tension test simulation.

Uniaxial tension can be achieved by modifying the velocity gradient of simple tension. Using \mathbf{X} and \mathbf{x} for the initial and the current location of a material point, respectively, the simple tension movement can be written



$$\mathbf{x} = \left(\begin{bmatrix} \exp(-0.5L_{33}t) & 0 & 0 \\ 0 & \exp(-0.5L_{33}t) & 0 \\ 0 & 0 & \exp(L_{33}t) \end{bmatrix} \mathbf{e}_i \otimes \mathbf{e}_j \right) [\mathbf{X}] \quad (5.1)$$

with

$$i, j = 1, 2, 3.$$

Since crystalline response to the loading is anisotropic the Taylor assumption for such deformation does not, as a rule, entail an uniaxial stress state. Therefore, we use a Newton procedure to iterate the proper velocity gradient tensor, \mathbf{L}_i , which produces a macroscopic simple tension stress state for the time step i . This means that the following equation should be solved

$$\mathbf{G}_i(\mathbf{L}_i) = \bar{\mathbf{T}}(\mathbf{L}_i) - \sigma_i \mathbf{e}_3 \otimes \mathbf{e}_3 = \mathbf{0}. \quad (5.2)$$

In this expression the uniaxial tension direction is along the \mathbf{e}_3 direction. From this equation the consistent tangent $\mathbf{J}_i = \frac{\partial \mathbf{G}_i}{\partial \mathbf{L}_i}$ can be derived as outlined in detail in the Appendix of this report. The algorithm of the iteration procedure consists of the following steps: First, one starts with a given initial value $\mathbf{L}_i^0 = \mathbf{L}$ and a time increment Δt_i . Second, \mathbf{G}_i^0 and \mathbf{J}_i^0 are calculated to find the new velocity gradient $\mathbf{L}_i^1 = \mathbf{L}_i^0 - (\mathbf{J}_i^0)^{-1}[\mathbf{G}_i^0]$. Third, the new value for \mathbf{G}_i^1 is calculated. Finally, one has to check whether $\|\mathbf{G}_i^1\| \leq \text{Err}$. If this applies the time step is finished. If it does not apply for a fixed iteration number the time step is reduced by a factor of 2 and the algorithm is repeated.

In this study the ratio η_j of the dissipation rate, P_{diss} , and the total deformation energy density rate, P_{total} , is used to express the deformation amount for the single crystal j

$$\eta_j = \left. \frac{P_{diss}}{P_{total}} \right|_j = \left. \frac{\text{tr}(\mathbf{T}\mathbf{L}_p)}{\text{tr}(\mathbf{T}\mathbf{L})} \right|_j. \quad (5.4)$$

For determining whether the polycrystal yields we use the volume average of this ratio according to



$$\bar{\eta} = \frac{\sum_{j=1}^N V_j \eta_j}{\sum_{j=1}^N V_j} \quad (5.5)$$

where V_j are the single volume elements.

We analyze the q -value along different directions to investigate the planar anisotropy of rolled copper sheets. The loading directions of the simple tension tests are screened by using the fixed longitudinal direction \mathbf{e}_3 and stepwise rotations about the normal direction of the rolling plane \mathbf{e}_1 using a rotation tensor \mathbf{R} . The new lattice position for the crystal i is given by

$$\tilde{\mathbf{F}}_i^R = \mathbf{R} \tilde{\mathbf{F}}_i \quad (5.6)$$

where $\tilde{\mathbf{F}}_i$ is the elastic part of the deformation gradient \mathbf{F}_i , which is not orthogonal after the rolling and the unloading deformations, and $\tilde{\mathbf{F}}_i^R$ is the new value of this tensor after the rotation. Conducting sheet normal rotations in 5° steps yields 19 separate simple tension test simulations which are sufficient to study the anisotropy of rolled sheets.



6 Evaluation of the texture predictions

Figs. 1 and 2 show that the introduction of a standard deviation for the velocity gradient by use of a pseudorandom distribution function drastically decreases the texture sharpness known from the classical Taylor theory. This can be attributed to the fact that the new approach considers the interaction of the grains at least in a statistical fashion as outlined above.

Some positions of the main texture components are also in better accordance with experimental data than the predictions of the classical Taylor theory, though the agreement is not yet sufficiently convincing.

For instance the position of the Brass component, as predicted by the modified Taylor model, is in better accord with the experiment when compared to the FC Taylor model. The scatter on the $\langle 110 \rangle$ texture fiber between the Goss and the Brass components, however, is larger than observed in experiment. The positions of the Copper and of the S components are in the new approach similar as in the Taylor FC simulation, but their sharpness is much smaller.

The observation that the agreement between the new Taylor model and the experimental data is not yet sufficiently good can in part be attributed to the fact that we introduced the interaction effect for the modification of the symmetric part of the velocity gradient tensor, but the corresponding pseudorandom modification of the skew symmetric part of this tensor was not included although it might be of relevance for the calculation of the reorientation rates.

Another aspect which offers room for improvement of the model is that we introduced the standard deviation equally for all components of the velocity gradient.



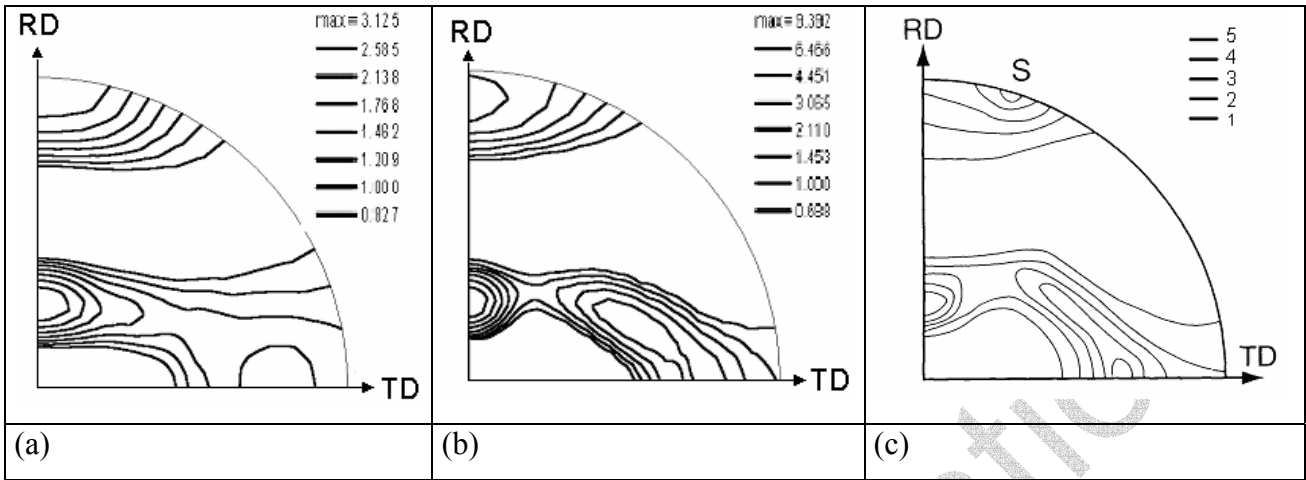


Fig. 1 {111} pole figures for (a) the modified Taylor model (standard deviation=0.0002, 90% thickness reduction); (b) Taylor FC model (90% thickness reduction); (c) Experimental data for rolled Cu [data taken from Kocks, 4], rolled to 96%.

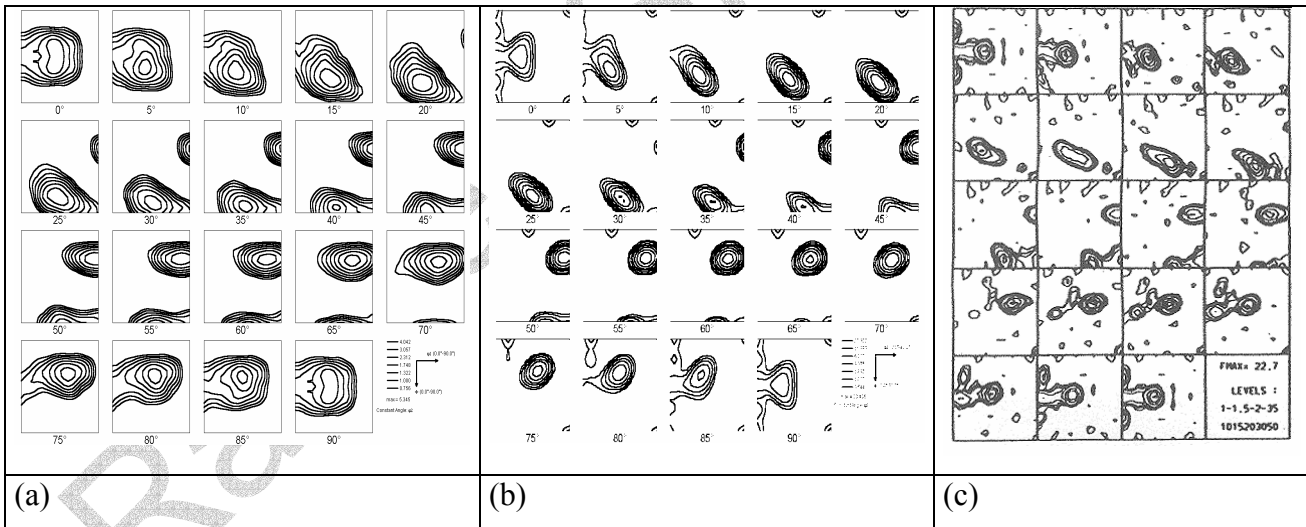


Fig. 2 Orientation distribution function for (a) the modified Taylor model (standard deviation=0.0002, 90% thickness reduction); (b) Taylor FC model (90% thickness reduction); (c) experimental data for Cu-2%Zn rolled to 96% thickness reduction [data taken from Savoie, 35]. The functions are given in the reduced Euler space in the form of $\Delta\phi_2=5^\circ$ sections running from $\phi_2=0^\circ$ to $\phi_2=90^\circ$.

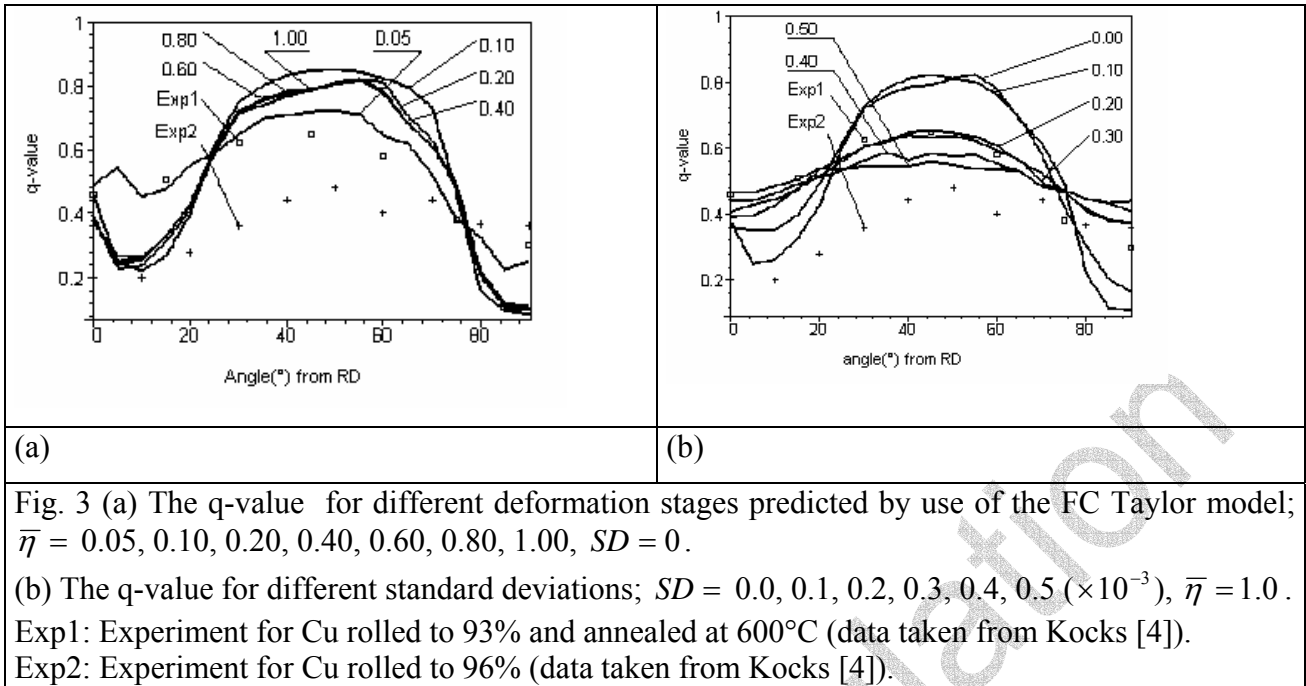


7 Evaluation of the anisotropy predictions

We studied the in-plane anisotropy for a rolled Copper sheet as a function of the preceding deformation by use of the new Taylor model. We use the volume average parameter $\bar{\eta}$ to describe the deformation. For purely elastic straining $\bar{\eta}$ is almost zero. For larger deformations it saturates at 1.0.

Fig. 3a shows the influence of the deformation on the q – value as a function of the angle between straining direction and the former rolling direction for a standard deviation $SD = 0$. When the deformation is small (e.g. $\bar{\eta} = 0.05$), only a small portion of the grains begins to yield while the others are loaded only into the elastic regime. The q – value does at this stage, therefore, not represent the complete plastic anisotropy of the rolled sheet. As the deformation increases the q – value gradually converges. The numerical result is based on the simulated texture shown in Fig. 2b. In Fig. 3b the simulated Lankford coefficients for different SD at $\bar{\eta} = 1.0$ are compared to experimental data taken from the work of Kocks [4]. The curve indicated by *Exp1* was a rolled and annealed Copper specimen while the curve indicated by *Exp2* was rolled and not subsequently heat treated. The comparison shows that the anisotropy predictions obtained by the modified Taylor model reveal a good agreement with the experimental data for angles above 50° . The discrepancy of experiment and simulation for angles below 50° can essentially be attributed to the deviation between the experimentally observed and simulated input textures. Fig. 3b also shows the influence of the standard deviation on the q – value as a function of the angle between straining direction and the former rolling direction. Although the match between experiments and simulations in Fig. 3b, such as for $SD = 0.0002 \sim 0.0005$ and $\bar{\eta} = 1.0$, is somewhat better than the FC Taylor model in Fig. 3a for $SD = 0$ and $\bar{\eta} = 1.0$ a principal shift of the predictions towards larger values is still apparent.





Conclusions

We presented a modified Taylor model which statistically considers grain interaction in a polycrystalline aggregate in terms of a standard deviation for the symmetric part of the velocity gradient. The model was solved by using a Newton iteration scheme. We simulated crystallographic rolling textures and the elastic-plastic anisotropy arising from uniaxial tension tests. The results reveal in part a good agreement with experimental data. In particular we observed a considerable drop in the predicted texture sharpness. The simulation results obtained for uniaxial tension showed that the texture sharpness has considerable influence on the plain anisotropy of rolled sheets.

Raabe - Simulation



REFERENCES

1. Van Houtte P. In: Preferred Orientations in Deformed Metals and Rocks. An Introduction of Modern Texture Analysis, Vol. Ed.: H. -R. Wenk. Academic Press, New York, 1985.
2. Aernoudt EP, Van Houtte P, Leffers T. Chapter 3 in: Deformation and Textures of Metals at Large Strain, Volume 6, Vol. ed.: H. Mughrabi: Plastic Deformation and Fracture of Materials of Materials Science and Technology — A Comprehensive Treatment, Ser. eds.: R. W. Cahn, P. Haasen, and E. J. Krämer. VCH, Weinheim. 1993.
3. Hosford WF. The Mechanics of Crystals and Textured Polycrystals. Oxford University Press 1993.
4. Kocks UF, Tóme CN, Wenk HR. Texture and Anisotropy, Cambridge University Press 1998.
5. Raabe D. Computational Materials Science, Wiley-VCH, Weinheim 1998.
6. Sachs GZ. Ver. Dtsch. Ing. 1928; 72:734.
7. Taylor GI. J. Inst. Metals 1938; 61:307.
8. Honneff H, Mecking H. Proc. 6th Int. Conf. on Tex. of Mat. ICOTOM 6, ed. S. Nagashima, Iron and Steel Inst. of Japan 347, 1981.
9. Van Houtte P. in Proc. 6th Int. Conf. on 'Texture of Materials' (ICOTOM 6), (ed. S. Nagashima), 428; 1981, Iron and Steel Inst. of Japan.
10. Kocks UF, Chandra H. Acta Metall. 1982; 30:695.
11. Raphanel JL, van Houtte P. Acta Metall. 1985; 33:1481.
12. Wagner, P., Ph. D. Thesis, RWTH Aachen, Germany, 1994.
13. Schmitter, U., Diplomarbeit RWTH Aachen, Germany, 1992.
14. Van Houtte P, Delannay L, Samajdar I. Textures Microstructures 1999; 31:109.
15. Raabe D. Acta Metall. 1995; 43:1023.
16. Raabe D. Mater. Sc. Eng. A 1995; 197:31.
17. Raabe D, Zhao Z., Mao W. Acta Mater. 2002; 50:4379.
18. Crumbach M, Pomana G, Wagner P, Gottstein G. Recrystallization and Grain Growth Proceedings of the First Joint International Conference Eds. G. Gottstein and D.A. Molodov, Springer-Verlag, Vol. II, 2001, 1053.
19. Mao W. Mater. Sc. Eng. A 1998; 257:171.
20. Molinari A, Canova GR, Ahzi S. Acta metall. 1987; 35:2983.
21. Sarma G, Dawson PR. Int. J. Plast. 1996 ; 12 :1023.



22. Bunge, HJ. Texture analysis in materials science. Butterworths, London, England 1982.
23. Wassermann G, Grewen J. Texturen metallischer Werkstoffe (in German), Springer-Verlag Berlin, Germany 1969.
24. Hirsch J, Lücke K. Acta Metall. 1988; 36: 2863.
25. Hölscher M, Raabe D., Lücke K. Acta metall. Mater. 1994; 42:879.
26. Rees DWA. Appl. Math. Modelling, 1997; 21:579.
27. Lankford WT, Snyder SC, Bausher JA. Trans. ASM 1950; 42:1197.
28. Kitamura K, Miyazaki S, Iwai H, Kohl M. Mater. Sc. Eng. A 1999; 273-275:758.
29. Lee WB, To S. J. Mater. Proc. Techn. 1995; 48:179.
30. Spolidor A. J. Mater. Sc. 1996; 31:5731.
31. Bertram A. Int. J. Plast. 1999; 15:353.
32. Raabe D, Sachtleber M, Zhao Z, Roters F, Zaefferer S. Acta Materialia 2001; 49:3433.
33. Sachtleber M, Zhao Z, Raabe D. Mater. Sc. Engin. A 2002; 336:81.
34. Engler O. Adv. Engin. Mater. 2002, 4:181
35. Savoie JF. Ph.D. Dissertation Thesis, RWTH Aachen, 1990.



Appendix : Derivation of the consistent tangent modulus

The volume average of Cauchy stress can be simplified for the case that every single crystal has the same volume

$$\bar{\mathbf{T}}(\mathbf{L}, \Delta t) = \frac{1}{N} \sum_{i=1}^N \mathbf{T}_i(\mathbf{L}, \Delta t). \quad (\text{A.1})$$

For every time step Δt the following equation should be satisfied for every single crystal

$$\mathbf{H}_i = \tilde{\mathbf{F}}_i^n(\mathbf{L}) - \tilde{\mathbf{F}}_i^{n-1} - \dot{\tilde{\mathbf{F}}}_i^n(\mathbf{L}, \tilde{\mathbf{F}}_i^n) \Delta t = \mathbf{0}. \quad (\text{A.2})$$

There are two variables $\tilde{\mathbf{F}}_i^n$ and \mathbf{L} in this function, so that their derivative relation can be set

$$\Delta \mathbf{H}_i = \frac{\Delta \mathbf{H}_i}{\Delta \tilde{\mathbf{F}}_i^n} \Delta \tilde{\mathbf{F}}_i^n + \frac{\Delta \mathbf{H}_i}{\Delta \mathbf{L}} \Delta \mathbf{L} = \mathbf{0} \quad (\text{A.3})$$

$$\frac{\Delta \tilde{\mathbf{F}}_i^n}{\Delta \mathbf{L}} = - \left(\frac{\Delta \mathbf{H}_i}{\Delta \tilde{\mathbf{F}}_i^n} \right)^{-1} \frac{\Delta \mathbf{H}_i}{\Delta \mathbf{L}} \quad (\text{A.3})$$

Based on these equations the consistent tangent module \mathbf{J} can be written as

$$\mathbf{G} = \bar{\mathbf{T}}(\mathbf{L}, \Delta t) - \bar{\mathbf{T}}_0 = \frac{1}{N} \sum_{i=1}^N \mathbf{T}_i(\mathbf{L}, \Delta t) - \bar{\mathbf{T}}_0 \quad (\text{A.4})$$

$$\mathbf{J} = \frac{\Delta \mathbf{G}}{\Delta \mathbf{L}} = \frac{\Delta \bar{\mathbf{T}}}{\Delta \mathbf{L}} = \frac{1}{N} \sum_{i=1}^N \frac{\Delta \mathbf{T}_i}{\Delta \mathbf{L}} = \frac{1}{N} \sum_{i=1}^N \frac{\Delta \mathbf{T}_i}{\Delta \tilde{\mathbf{F}}_i^n} \frac{\Delta \tilde{\mathbf{F}}_i^n}{\Delta \mathbf{L}} \quad (\text{A.5})$$



With this result the equation (2.3) can be simplified for small elastic deformations

$$\mathbf{T} \approx \tilde{\mathbf{F}} \tilde{\mathbf{K}} \left[\frac{1}{2} (\tilde{\mathbf{F}}^T \tilde{\mathbf{F}} - \mathbf{I}) \right] \tilde{\mathbf{F}}^T \quad (\text{A.6})$$

and the derivative of \mathbf{T} with respect of $\tilde{\mathbf{F}}$ is

$$\left(\frac{d\mathbf{T}}{d\tilde{\mathbf{F}}} \right)_{abcd} = \delta_{ac} \left(\tilde{\mathbf{K}} \left[\frac{1}{2} (\tilde{\mathbf{F}}^T \tilde{\mathbf{F}} - \mathbf{I}) \right] \tilde{\mathbf{F}}^T \right)_{db} + \left(\tilde{\mathbf{F}} \tilde{\mathbf{K}} \left[\frac{1}{2} (\tilde{\mathbf{F}}^T \tilde{\mathbf{F}} - \mathbf{I}) \right] \right)_{ad} \delta_{bc} + \tilde{F}_{ak} \tilde{K}_{kldn} \tilde{F}_{cn} \tilde{F}_{bl} \quad (\text{A.7})$$

with

$$\delta_{ij} = \begin{cases} 1 & i = j \\ 0 & i \neq j \end{cases} .$$

Replacing \mathbf{T} by \mathbf{T}_i and $\tilde{\mathbf{F}}$ by $\tilde{\mathbf{F}}_i$ in equation (A.7) and combining with equation (A.5), one can get the consistent tangent module \mathbf{J} in explicit form.

